On Dynamical/Statistical Initialization for Numerical Weather Prediction

WILLIAM BLUMEN

Astro-Geophysics Department, University of Colorado, Boulder 80309

(Manuscript received 7 April 1976, in revised form 12 August 1976)

ABSTRACT

A dynamical/statistical approach to initialization that is compatible with the dynamics of potential vorticity conservation is proposed. This approach consists of combining weighted assimilation, which minimizes the analysis error by means of linear regression, with a dynamical constraint imposed by this conservation principle. As a consequence, the initial analysis is shown to be optimal *and* dynamically compatible with the forecast model used in the present study.

Two situations that contribute to error growth in numerical prediction models are considered: 1) differences in the phase propagation speed of the model disturbance relative to that of the true or control state and 2) distortion of the initial error field by nonlinear wave interactions. In each case results obtained with the proposed dynamical/statistical initialization are compared with results from weighted assimilation using uncorrelated observational errors and from initialization by direct use of error-contaminated observations. These comparisons demonstrate the theoretical advantage of using an initialization scheme that is compatible with the model dynamics. However, it is pointed out that practical aspects involving additional computations and use of data from mixed observing systems have not been taken into account.

1. Introduction

The guiding principles that have propelled activities associated with numerical weather prediction, from its inception to its present state, are enmeshed in the tenet that the atmosphere is a deterministic system governed by macroscale physical laws. Much effort has been expended on the development of mathematical models of the atmosphere with concomitant initial and boundary conditions. Research by modelling groups to reduce forecast error variance has primarily focussed on the reduction of numerical truncation and the simulation of dynamical processes at an ever-increasing level of detail and complexity. There is, perhaps, universal agreement that improvement in atmospheric model dynamics is a viable research goal and that numerical algorithms, needed to implement a forecast, should keep pace with both the computational requirements of the model and increased computer capabilities. However, there is not necessarily universal agreement on the appropriate path that should be taken in future model development for numerical prediction. Paltridge (1975), for example, suggests that the prevailing approach to model development "is at variance with the basic philosophy of physics which, when faced with a complex problem, searches for simple laws which may govern the overall situation. Ideally, such laws should be simple in both concept and application." Moreover, in view of the inherent constraint placed on deterministic prediction by the use of error-prone observations with imperfect dynamical models, combined dynamical/statistical approaches have emerged as an attractive area for research in data assimilation and in model development.

The present investigation is directed toward initialization or data assimilation. The approach combines the usual techniques of objective analysis which minimizes the analysis error by means of linear regression, with dynamical constraints imposed by the model. Previous work in the field of dynamical/statistical data assimilation has been reviewed recently by Bengtsson (1975). It appears that methods in current use only apply dynamical constraints in the form of balance conditions or *initial* accelerations, calculated from the equations of motion. The former approach has been followed by Rutherford (1973) and Schlatter (1975), for example, who assumed that forecast error covariances are geostrophically related and that observational errors are random and uncorrelated. Schlatter presents evidence to substantiate the geostrophic error covariance assumption but, as will be shown, the restriction placed on the observational errors is not necessarily an appropriate constraint to be used with geostrophic balance. Initial accelerations have been incorporated by Lewis and Grayson (1972) using Sasaki's (1958) variational procedure. While this approach is less restrictive than that provided by balanced conditions alone, the variational procedure is not widely used as an operational tool at this time.

In summary, current procedures of data assimilation are directed toward an optimal *analysis* of the observed

fields under constraints of dynamical model consistency. It will be shown that an optimal analysis does not necessarily guarantee an optimal forecast even when a linear dynamical model is employed. The problem is in defining what constitutes an optimal analysis. As noted, current procedures attempt to impose dynamical constraints at a particular time. The present approach is one that optimizes the initial meteorological fields in a manner that is compatible with the dynamics governing the evolution of these fields during the forecast period: conservation of potential vorticity provides the fundamental dynamical principle. Although attention is directed here to the dynamics of mid-latitude disturbances, the underlying principle could be useful in the design of tropical analysis schemes. However, a conservation principle that is appropriate at low latitudes has not yet been established.

The present method was first developed from a linear barotropic model or, equivalently, a shallow-water model in which the dynamics of the geostrophic adjustment process is described by dispersion of gravity-inertia waves, leaving a steady geostrophic flow (Blumen, 1976c). The present paper is intended to provide a more general development in which the evolution of the geostrophic flow is governed by the nonlinear quasigeostrophic forecast equation. This development appears in Section 2. Results from the previous study are then summarized in Section 3. These results are used to aid in the interpretation of rms prediction errors obtained from application of the present dynamical/statistical initialization scheme to:

1. Forecast errors associated with both the observational errors and with an error in the phase propagation speed of the model disturbance relative to that of a control state (Section 4).
2. Forecast errors associated with nonlinear distortion of observational errors (Section 5).

In each case results obtained using the present scheme are compared with results obtained from optimal initialization using random uncorrelated observational errors and from initialization by direct replacement with error-contaminated observations. These comparisons demonstrate the theoretical advantage of using an initialization scheme that is compatible with the dynamics of the model. Some additional remarks based on this result appear in Section 6.

2. Theory

The barotropic model used in the present study has been developed and discussed previously by the author (Blumen, 1972, 1975a). The basic physical principle underlying the present development is conservation of potential vorticity. As a consequence, the present initialization scheme would be most appropriately applied to short-range prediction or when new data are assimilated frequently, say, within a period $\tau \lesssim 24$ h.

The present model admits two types of wave solutions, gravity-inertia waves and planetary or Rossby waves. The former class is characterized by higher frequencies than the latter. As a consequence a two time-scale approach provides a consistent expansion procedure to separate the set of equations governing the dynamics of each class of waves. In the lowest-order system, the high-frequency ageostrophic gravity-inertia waves and relatively low-frequency quasi-geostrophic planetary waves are coupled only through the initial conditions. Interactions between each class of waves appear at higher order. Numerical experiments by Williamson and Kasahara (1971), for example, do not indicate that interactions between gravity-inertia waves and planetary waves are a significant source of forecast error for short-range prediction. Consequently, only the lowest-order system will be retained. The fact that ageostrophic and quasi-geostrophic wave motions evolve independently, once the initial conditions are satisfied, emerges as a focal point in the following analysis.

The nondimensional zero-order streamfunction ψ_0 may be expressed as

$$\psi_0(x,y,T,\tau)=\Psi(x,y,\tau)+\psi(x,y,T,\tau), \tag{1}$$

where Ψ and ψ denote the geostrophic and ageostrophic streamfunctions, respectively, and x, y are Cartesian coordinates directed eastward and northward. The fast time is $T=t$ and the slow time is $\tau=\mathrm{Ro}t$, where t is time, nondimensionalized by the Coriolis parameter $f=f_0$; $\mathrm{Ro}=U_0/f_0L\sim 10^{-1}$, which represents the characteristic ratio of the two time scales for values of zonal wind U_0 and quarter wavelength L, typical of mid-latitude synoptic-scale flow.

The quasi-geostrophic flow is governed by conservation of potential vorticity

$$\left(\frac{\partial}{\partial\tau}-\frac{\partial\Psi}{\partial y}\frac{\partial}{\partial x}+\frac{\partial\Psi}{\partial x}\frac{\partial}{\partial y}\right)\Omega_0=0, \tag{2}$$

where the potential vorticity is given by

$$\Omega_0=(\Delta-\lambda^{-2})\Psi+\beta y, \tag{3}$$

$\Delta=\partial^2/\partial x^2+\partial^2/\partial y^2$, $\beta=df/dy=$ constant, and λ is the nondimensional radius of deformation

$$\lambda\equiv(g'D_0)^{\frac{1}{2}}f_0^{-1}L^{-1} \tag{4}$$

defined by means of reduced gravity g' and layer depth D_0. Typical atmospheric values will be considered later.

The wave equation that governs the ageostrophic motion is provided by

$$\left(\frac{\partial^2}{\partial T^2}+1-\lambda^2\Delta\right)\psi=0. \tag{5}$$

The potential vorticity of the ageostrophic motion is

identically zero, i.e.,

$$\Delta\psi-\lambda^{-2}\pi=0, \tag{6}$$

where $\pi=\pi(x,y,T,\tau)$ denotes the ageostrophic height deviation from the constant undisturbed depth D_0 or the surface pressure deviation in a barotropic model. This important property [Eq. (6)] of the ageostrophic motion will be exploited in the design of the proposed initialization procedure. In effect, (6) is a conservation principle for ageostrophic accelerations: at any time T or τ, ψ and π are constrained by a balance condition. Consequently, if (6) can be introduced into the initialization procedure the information provided by the initial accelerations is preserved throughout the time history of the flow. In other words, the initialization procedure would be compatible with the model dynamics. The next step is to develop a rationale for the optimal use of (6).

Linear regression has often been used as a convenient tool to minimize analysis error by providing appropriate weights to both the forecast and the observed fields. These weighting factors are expressed in terms of the relative errors in each of these fields. In application, the best estimate of a meteorological variable at a grid point is determined by means of a weighted linear combination of the difference between the forecast and observed fields at a discrete set of observing stations surrounding the grid point. Here interpolation is unnecessary, since the present model is based on the availability of a continuous spatial distribution of data. Consequently the best estimates of the initial streamfield and height (or pressure) fields are provided by

$$\psi^e=\psi^t[1-(1-\mu_\psi)\epsilon_\psi^p-\mu_\psi\epsilon_\psi^o], \tag{7}$$

$$\pi^e=\pi^t[1-(1-\mu_\pi)\epsilon_\pi^p-\mu_\pi\epsilon_\pi^o], \tag{8}$$

where the superscripts denote the estimate (e), the true value (t), the prediction (p) and the observation (o); the errors (ϵ) and weight factors (μ) are tagged with the subscript ψ or π to indicate association with one or the other field. For convenience, the initial errors in ψ and π have all been expressed in the form

$$\epsilon_\psi^q=\frac{\psi^t-\psi^o}{\psi^t}, \tag{9}$$

and similarly for prediction errors.

The theoretical basis of the proposed initialization procedure is not affected by the simple form assumed in (7) and (8), although operational requirements would dictate use of the discrete form of the interpolation formulas. Another obvious simplification is the use of the streamfunction rather than velocity components, which are normally observed in practice.

If the forecast and observational errors are uncorrelated with each other then the usual least squares minimization yields

$$\left\langle\left|\frac{\psi^t-\psi^e}{\psi^t}\right|^2\right\rangle\Bigg|_{\min}=(1-\mu_\psi)\langle|\epsilon_\psi^p|^2\rangle$$

$$=\mu_\psi\langle|\epsilon_\psi^o|^2\rangle, \tag{10}$$

$$\left\langle\left|\frac{\pi^t-\pi^e}{\pi^t}\right|^2\right\rangle\Bigg|_{\min}=(1-\mu_\pi)\langle|\epsilon_\pi^p|^2\rangle$$

$$=\mu_\pi\langle|\epsilon_\pi^o|^2\rangle, \tag{11}$$

where the angle brackets denote a statistical average and the weight factors are given by

$$\mu_\psi=\frac{\langle|\epsilon_\psi^p|^2\rangle}{\langle|\epsilon_\psi^p|^2\rangle+\langle|\epsilon_\psi^o|^2\rangle}, \tag{12}$$

$$\mu_\pi=\frac{\langle|\epsilon_\pi^p|^2\rangle}{\langle|\epsilon_\pi^p|^2\rangle+\langle|\epsilon_\pi^o|^2\rangle}. \tag{13}$$

These expressions have been derived by Rutherford (1972), among others, and were applied to the present model in a previous study (Blumen, 1975b).

The optimal analyses of both the streamfield and the pressure field are provided by (7) and (8), provided that the weight factors are (12) and (13). Some model dynamics is built into the analyses fields through the use of forecast information. Additional dynamics may be introduced by assuming that prediction errors in the height and wind fields are geostrophically related, i.e.,

$$\langle|\epsilon_\pi^p|^2\rangle=\langle|\epsilon_\psi^p|^2\rangle, \tag{14}$$

and that the observational errors are assumed to be statistically independent. These assumptions have been used by Rutherford (1973) and Schlatter (1975), for example, to simplify covariance computations that appear when multivariate representations of (7) and (8) are used. Correlations based on the use of (14) were computed by Schlatter and compared with those based on radiosonde data. Reasonably good qualitative agreement was found between the comparable fields. Nonetheless, initialization by means of (7) and (8) with weight factors (12) and (13) is fundamentally tied to an optimal analysis. The dynamical consequences of such a choice, for a particular model, have not been clarified. The present purpose is to critically examine a dynamical consequence of incorporating geostrophic prediction error statistics into the initial analysis scheme. The dynamical model is provided by (2), (5) and (6).

For the moment, we shall set aside the statistical approach to concentrate on the purely dynamical content of the present model. As noted, the zero-order fields ψ_0 and π_0 may be expressed in terms of geostrophic

and ageostrophic components

$$\psi_0=\Psi+\psi, \tag{15}$$

$$\pi_0=\Pi+\pi, \tag{16}$$

which satisfy (2), (5) and (6). The ageostrophic scalar potential

$$\phi_0=\phi(x,y,T,\tau) \tag{17}$$

also satisfies (5). The geostrophic and ageostrophic velocity fields are given by

$$\mathbf{V}=\mathbf{k}\times\nabla\Psi=\mathbf{k}\times\nabla\Pi, \tag{18}$$

$$\mathbf{v}=\nabla\phi+\mathbf{k}\times\nabla\psi, \tag{19}$$

where $\mathbf{k}$ is a unit vector, normal to the (x,y) plane, and ∇ denotes the two-dimensional gradient operator.

Blumen (1975a, Section 2a) has shown by the use of (6) that the sum of the kinetic plus available potential energy of the initial field can be separated into a geostrophic and ageostrophic part, i.e.

$$\mathcal{E}(\tau=T=0)=\frac{1}{2}\int\int_S \{|\mathbf{V}|^2+\lambda^{-2}\Pi^2+|\mathbf{v}|^2+\lambda^{-2}\pi^2\}dxdy, \tag{20}$$

where S is the region of flow. If the region is infinitely large, the velocity components vanish at infinity. If it is bounded, we choose $\Psi=0$ on the boundary, supplemented by conservation of circulation to provide well-posed boundary conditions for doubly-connected regions (Arnold, 1965). Moreover, the geostrophic and ageostrophic flow fields individually conserve their initial energy, although (2) shows that nonlinear interactions between the quasi-geostrophic modes may occur.

As a consequence of the separability property of the present model solutions, the total energy of the *ageostrophic* flow may be expressed as

$$\mathcal{E}'(\tau=T=0)=\frac{1}{2}\int\int_S \left\{\left[\frac{\partial}{\partial x}(\psi_0-\Psi)\right]^2+\left[\frac{\partial}{\partial y}(\psi_0-\Psi)\right]^2+\left(\frac{\partial\phi_0}{\partial x}\right)^2+\left(\frac{\partial\phi_0}{\partial y}\right)^2+\lambda^{-2}(\pi_0-\Pi)^2\right\}dxdy, \tag{21}$$

where $\psi=\psi_0-\Psi$ and $\Psi=\Pi$. Dikii (1969) has established a *minimum energy principle* that applies to the present model. [A proof, based on the variation of $\mathcal{E}'$ with respect to Ψ, appears in Blumen (1972, Section F(1a)]. The essence of this principle is that the adaptation of the flow occurs in such a way that the ageostrophic motion has the least energy of all possible differences between the initial and quasi-geostrophic states. Since the ageostrophic flow conserves its initial energy [Blumen, 1975a, Eq. (23)], the ageostrophic flow will always remain in a minimum energy state. Alternatively, if the maximum amount of energy available from the initial state is partitioned to geostrophic flow, potential vorticity is conserved. This conservation principle has been expressed by (2) and (6).

Suppose that the initial fields ψ_0 and π_0 are represented as

$$\psi_0=(1-\epsilon_\psi)\psi^t, \tag{22}$$

$$\pi_0=(1-\epsilon_\pi)\pi^t, \tag{23}$$

where ϵ_ψ and ϵ_π are the total error fields represented as in (9). Without loss of generality, we set $\phi_0=0$. Following the previous guidelines, both the true and error fields may be further subdivided into geostrophic and ageostrophic components; we assume that the errors are random variables which are not correlated with the true values. Then, in analogy with (21), the average ageostrophic error energy may be expressed as

$$\langle\mathcal{E}^A\rangle=\frac{1}{2}\int\int_S \left[\left\langle\left(\frac{\partial\epsilon_\psi^A}{\partial x}\right)^2\right\rangle+\left\langle\left(\frac{\partial\epsilon_\psi^A}{\partial y}\right)^2\right\rangle+\lambda^{-2}\langle(\epsilon_\pi^A)^2\rangle\right]dxdy, \tag{24}$$

where $\epsilon_\psi^A=\epsilon_\psi-\epsilon_\psi^G$ and $\epsilon_\pi^A=\epsilon_\pi-\epsilon_\pi^G$ are ageostrophic errors while ϵ_ψ^G and ϵ_π^G are geostrophic errors that are related through the balance condition (14). Consequently, $\langle\mathcal{E}^A\rangle$ may be varied with respect to ϵ_ψ^G to establish a minimum energy principle for the error fields that is identical to Dikii's principle stated above. In summary, if the ageostrophic error is a minimum relative to the geostrophic error, the potential vorticity of the error field is conserved. In particular,

$$\Delta\epsilon_\psi^A-\lambda^{-2}\epsilon_\pi^A=0. \tag{25}$$

Thus, if geostrophic prediction errors are introduced, as in (14), the observational errors ϵ_ψ^o and ϵ_π^o must be related through potential vorticity conservation [Eq. (25)] to provide dynamical consistency. This constraint is a natural consequence of the minimum energy principle associated with the optimal partition of energy in the present dynamical model. The assumption of statistical independence between the observational errors is incompatible with the model dynamics.

It is now possible to evaluate the weighting factors (12) and (13) which minimize the analysis errors, by means of dynamical constraints (14) and (25) that minimize the observational errors in a manner that is consistent with the evolution of the flow.

3. Application of the theory

The initial conditions for the solution of (2) and (5) have been set down by Blumen (1976a). At $\tau=T=0$, these conditions are

$$\psi_0(x,y)=\Psi(x,y,0)+\psi(x,y,0,0), \tag{26}$$

$$\partial\Delta\psi/\partial T=-\Delta\phi_0, \tag{27}$$

$$\partial^2\Delta\psi/\partial T^2=-\Delta(\psi_0-\pi_0), \tag{28}$$

where ψ_0, π_0 and ϕ_0 are given by (15), (16) and (17). The determination of $\Psi(x,y,0)$ is not affected by condition (27). However, gravity-inertia waves owe their existence to the imbalances provided by (27) and (28). After the initial conditions are satisfied, only the quasi-geostrophic solution will be examined. The "fast" waves, described by (5), are removed to simulate damping processes, either physical or numerical, that are present in numerical models of the atmosphere.

In order to examine prediction errors the true state of the model atmosphere, that satisfies (2), will be represented by

$$\psi^t(x,y,\tau)=\hat{\psi}\exp[i(kx+\sigma\tau)+ily], \tag{29}$$

where $\hat{\psi}$ is a constant amplitude and the wave frequency is given by

$$\sigma=\frac{k\beta}{\kappa^2+\lambda^{-2}}, \tag{30}$$

β and λ are defined by (3) and (4) and $\kappa^2=k^2+l^2$ denotes the sum of the squares of the (x,y) wavenumbers. The ageostrophic motion, including the error fields, may also be decomposed into Fourier space. Consequently, (25) reduces to

$$\epsilon_\psi^o=-\frac{a}{1-a}\epsilon_\pi^o, \tag{31}$$

where ϵ_ψ^o and ϵ_π^o are given by (9) and $a=[1+(\kappa\lambda)^2]^{-1}$. Since the errors are assumed to be random variables, the mean square errors are related through (31) and expressible as

$$\langle|\epsilon_\psi^o|^2\rangle=\left(\frac{a}{1-a}\right)^2\langle|\epsilon_\pi^o|^2\rangle. \tag{32}$$

Generally, $\langle|\epsilon_\psi^o|^2\rangle$ and $\langle|\epsilon_\pi^o|^2\rangle$ would be about the same order of magnitude $O(10^{-1})$ for typical observing systems. In order to make use of error information in an optimal manner, in terms of both the analysis and dynamics, the error fields are constrained to satisfy (14) and (32). Although these constraints are tied to the present model, previous applications appear to indicate that this dynamical model does capture the essence of some error growth processes in primitive equation models of the atmosphere.

The present goal is to reduce error growth by use of weighted assimilation with weight factors (12) and (13) evaluated with (14) and (32). Since it has been assumed that $\langle|\epsilon_\psi^o|^2\rangle\sim\langle|\epsilon_\pi^o|^2\rangle$,

$$\mu_\psi=\frac{\langle|\epsilon_\psi^p|^2\rangle}{\langle|\epsilon_\psi^p|^2\rangle+\left(\frac{a}{1-a}\right)^2\langle|\epsilon_\pi^o|^2\rangle} \tag{33}$$

when $0\leqslant a\leqslant 0.5$ and μ_π is provided by (13) with $\langle|\epsilon_\psi^p|^2\rangle=\langle|\epsilon_\pi^p|^2\rangle$. For larger scales of motion, $0.5\leqslant a\leqslant 1$, μ_ψ is given by (12) and

$$\mu_\pi=\frac{\langle|\epsilon_\psi^p|^2\rangle}{\langle|\epsilon_\psi^p|^2\rangle+\left(\frac{1-a}{a}\right)^2\langle|\epsilon_\psi^o|^2\rangle}. \tag{34}$$

Under the present assumptions, the weight factors (33) and (34) form a symmetric function of a; it is not necessary, however, that they do so. The values of a over which one or the other weight factor is to be used will depend on the actual spectral distribution of observational errors. This information is not generally known for meteorological observing systems.

One initial condition $\Psi(x,y,0)$ is required to solve (2). This is determined from (26) and (28), using (7) and (8) for the evaluation of ψ_0 and π_0. This procedure has been presented in detail by Blumen (1975a, Section 2b). The result is

$$\Psi(x,y,0)=\psi^t\{1-[(1-a)(1-\mu_\psi)+a(1-\mu_\pi)]\epsilon_\psi^p-[(1-a)\mu_\psi\epsilon_\psi^o+a\mu_\pi\epsilon_\pi^o]\}. \tag{35}$$

This initialization procedure has been applied by Blumen (1976c) to the simple case when the geostrophic solution is a steady current $\Psi(x,y)$. The root mean square (rms) geostrophic forecast errors

$$(\langle|\epsilon_\Psi|^2\rangle)^{\frac{1}{2}}=\left(\left\langle\left|\frac{\psi^t-\Psi}{\psi^t}\right|^2\right\rangle\right)^{\frac{1}{2}} \tag{36}$$

have been determined for three cases:

a. Weighted assimilation with correlated observational errors given by (32).

b. Weighted assimilation with statistically independent observational errors.

c. Direct assimilation of observations with statistically independent errors.

The latter case formally corresponds to setting $\mu_\psi=\mu_\pi=1$ in (35). Since the geostrophic solution is stationary, the initial and final states coincide, $\Psi(x,y,\infty)=\Psi(x,y,0)$. The rms errors, computed from (35), that correspond to the three cases above are:

CASE a

$$(\langle|\epsilon_\Psi|^2\rangle)^{\frac{1}{2}}=\{[(1-a)(1-\mu_\psi)+a(1-\mu_\pi)]^2\langle|\epsilon_\psi^p|^2\rangle+a^2[\mu_\pi-\mu_\psi]^2\langle|\epsilon_\pi^o|^2\rangle\}^{\frac{1}{2}}, \tag{37a}$$

CASE b

$$(\langle|\epsilon_\Psi|^2\rangle)^{\frac{1}{2}}=\{[(1-a)(1-\mu_\psi)+a(1-\mu_\pi)]^2\langle|\epsilon_\psi^p|^2\rangle+(1-a)^2\mu_\psi^2\langle|\epsilon_\psi^o|^2\rangle+a^2\mu_\pi^2\langle|\epsilon_\pi^o|^2\rangle\}^{\frac{1}{2}}, \tag{37b}$$

CASE c

$$(\langle|\epsilon_\Psi|^2\rangle)^{\frac{1}{2}}=\{(1-a)^2\langle|\epsilon_\psi^o|^2\rangle+a^2\langle|\epsilon_\pi^o|^2\rangle\}^{\frac{1}{2}}. \tag{37c}$$

The expressions are symmetric about $a=0.5$, as noted earlier. The weight factors in (37a) are given by (33) and (13) and by (12) and (13) in (37b).

TABLE 1. Value of $a=[1+(\kappa\lambda)^2]^{-1}$ appropriate under the restrictions of this analyses. The evaluations in the last two columns have been carried out using the characteristic values provided in the text but assuming, in each case, that $L=L_x/4$ is the characteristic length scale. The earth's radius is $r_e=6{,}371$ km and $\mathrm{Ro}=U/f_0L$, where $U=15.7$ m s^{-1} and $f_0=10^{-4}$ s^{-1}.

a	$L_x\times10^3$ (km)	L/r_e	Ro
0	0	—	
0.1	2094	0.082	0.30
0.2	3142	0.123	0.20
0.3	4113	0.1614	0.15
0.4	5130	0.201	0.12
0.5	6283	0.246	0.10
0.6	7695	0.302	0.08
0.7	9598	0.377	0.065
0.8	12 566	0.493	0.05
0.9	18 850	0.740	0.03
1.0	∞	—	—

The characteristic parameter values used for normalization were chosen to yield $\lambda^2(k^2+l^2)=(\lambda\kappa)^2=1$, $a=0.5$. These values, typical of midlatitude flow, are

$$\left.\begin{aligned} &L=L_x/4=L_y/4=(\pi/2)\times10^6\ \mathrm{m}\\ &k=l=2\pi L/L_x=\pi/2,\quad g'=0.625\ \mathrm{m\ s^{-1}}\\ &D_0=8\times10^3\ \mathrm{m},\quad f_0=10^{-4}\ \mathrm{s^{-1}}\end{aligned}\right\}.$$

Table 1 provides information on the range of a that may be appropriately considered under the restrictions that $\mathrm{Ro}\sim10^{-1}$ and $L/r_e\sim\mathrm{Ro}$, where r_e denotes the radius of the earth. This range is $0.1<a<0.7$, for the parameter values above.

Comparisons of the rms errors (37a,b,c) are shown in Figs. 1, 2 and 3. The principal results are:

(i) Weighted assimilation always reduces the forecast error, with the maximum reduction associated with case a: observational errors that satisfy potential vorticity conservation. The dynamical consequences of this latter case are most evident toward the short-wave part of the spectrum ($a\ll1$) and, by symmetry, toward the long wave part of the spectrum ($a\lesssim1$).

(ii) The relative maxima in the forecast errors, shown in Fig. 3, occur when $\langle|\epsilon_\psi^o|^2\rangle=\langle|\epsilon_\psi^p|^2\rangle$ which may easily be established from (37a).

The results obtained in the present case provide an overly optimistic view of the value of the initialization scheme that incorporates both dynamical constraints (14) and (32). No dynamical error growth occurs—all the error is associated with initialization. However, it is apparent from the figures that the initial "analysis," provided by linear regression, is not optimal until appropriate dynamical constraints are incorporated.

4. Phase errors

Dynamical error growth will be examined for two situations that are responsible, in part, for error growth in numerical prediction models. The propagation speed of wave disturbances is not, in general, predicted accurately by numerical models. A quantitative evaluation of error growth characteristics associated with phase differences has been presented by Blumen (1975a,b). In this section, the control of these errors by dynamical/statistical data assimilation will be con-

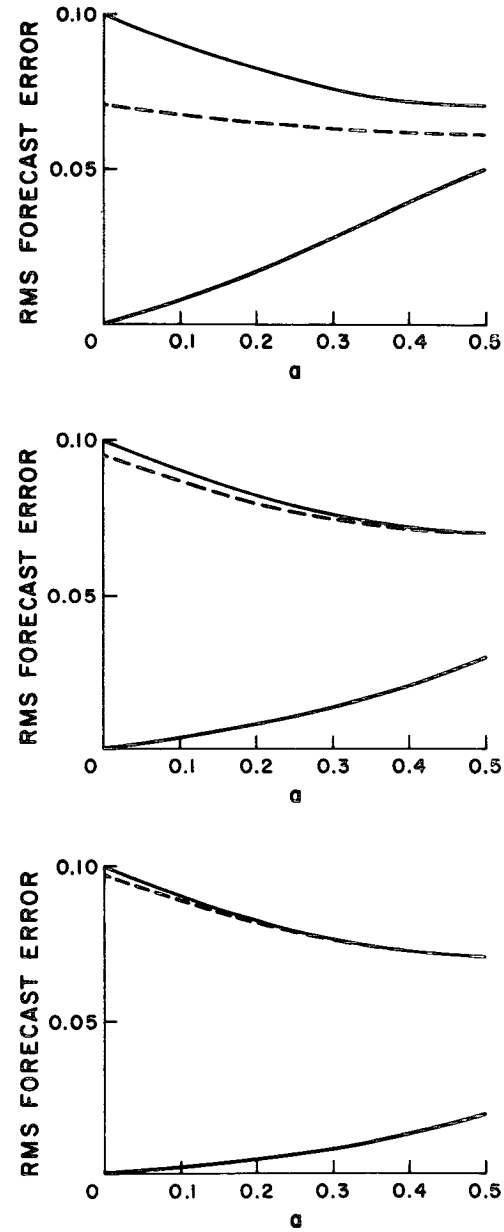

FIG. 1. Root-mean-square geostrophic forecast errors as a function of a, evaluated in Table 1. The curves correspond to weighted assimilation with both (case a) ageostrophically related observational errors (thick solid lines) and (case b) statistically independent observational errors (dashed lines); (case c) direct assimilation of observations with statistically independent errors is shown by the thin solid curve. The rms observational error is $(\langle|\epsilon_\psi^o|^2\rangle)^{\frac{1}{2}}=(\langle|\epsilon_\pi^o|^2\rangle)^{\frac{1}{2}}=0.1$. The initial forecast error is $(\langle|\epsilon_\psi^p|^2\rangle)^{\frac{1}{2}}=0.1$ (top), 0.3 (middle) and 0.5 (bottom).

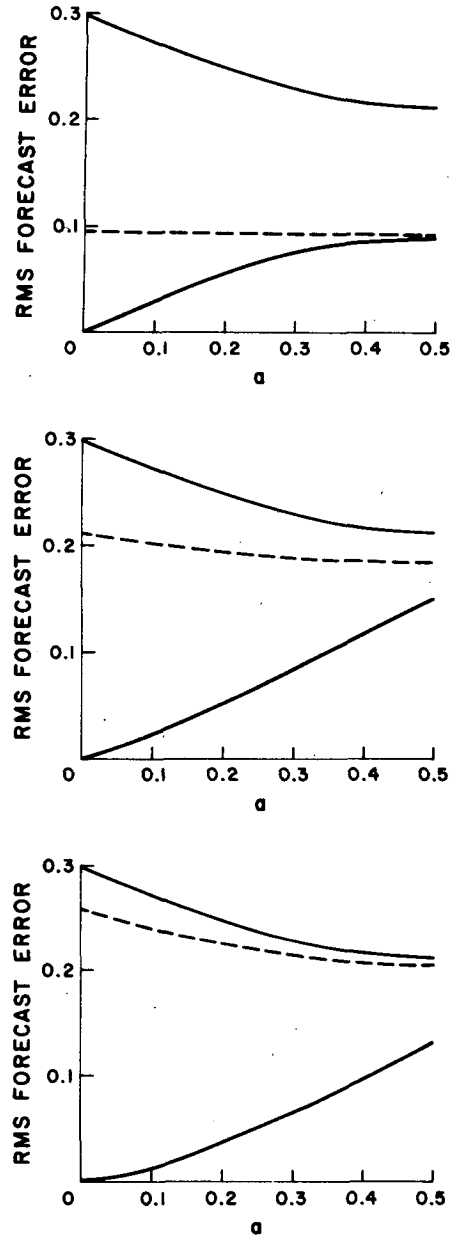

FIG. 2. As in Fig. 1 except $(\langle|\epsilon_\psi^o|^2\rangle)^{\frac{1}{2}}=(\langle|\epsilon_\pi^o|^2\rangle)^{\frac{1}{2}}=0.3$.

sidered. In the following section, the ability of the present scheme to control error growth associated with nonlinear wave interactions will be taken up.

The true state is represented by (29) and (30). The quasi-geostrophic forecast is made with (2) but the model dynamics are imperfectly represented by a radius of deformation $\lambda_\epsilon \neq \lambda$. Consequently, the wave frequencies are not equal, $\sigma_\epsilon \neq \sigma$, where

$$\sigma_\epsilon = \frac{k\beta}{\kappa^2+\lambda_\epsilon^{-2}}. \tag{38}$$

Data assimilation at constant time intervals $\Delta\tau$ will be undertaken in order to assess the ability of different initializations to control phase errors that are characterized by the nondimensional parameter

$$\theta = (\sigma-\sigma_\epsilon)\Delta\tau. \tag{39}$$

As in Section 3, case a corresponds to weighted assimilation with correlated observational errors and case b corresponds to weighted assimilation with statistically independent observational errors. Comparisons will be made between these two cases and with case c which is a variant of the case treated by Blumen (1975a,b). At each period $n\Delta\tau (n=0, 1, \ldots N)$ the streamfield is updated with observed values

$$\psi^o = \psi^t(1-\epsilon_\psi^o), \tag{40}$$

where ϵ_ψ^o denotes the random error at $n\Delta\tau$ while the initial height or pressure field is the predicted field at time $n\Delta\tau$, $\pi^p=\pi^p(n\Delta\tau)$. For simplicity, the phase error will be taken as constant. The asymptotic rms forecast error is

$$\lim_{N\to\infty} (\langle|\epsilon_\Psi^{(N)}|^2\rangle)^{\frac{1}{2}} \equiv E^{(\infty)}, \tag{41}$$

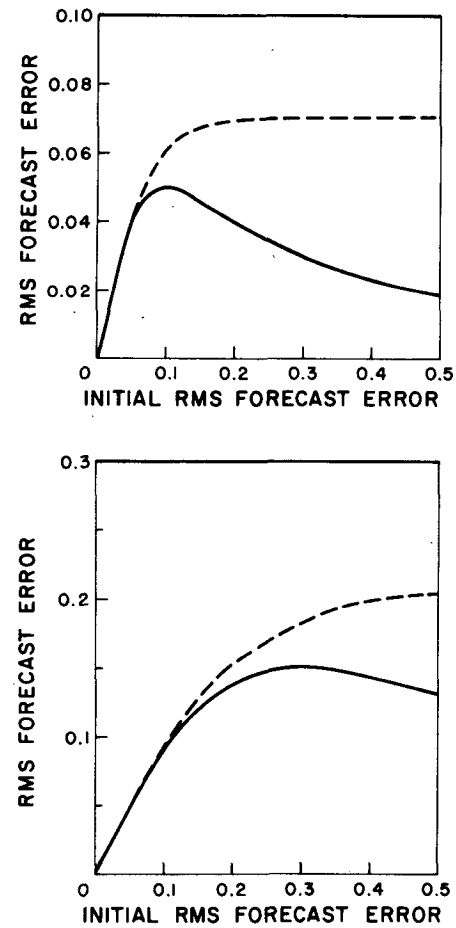

FIG. 3. Root-mean-square geostrophic forecast error as a function of the initial forecast error $(\langle|\epsilon_\psi^o|^2\rangle)^{\frac{1}{2}}$. The curves are designated as in Fig. 1. The observational error $(\langle|\epsilon_\psi^o|^2\rangle)^{\frac{1}{2}}=(\langle|\epsilon_\pi^o|^2\rangle)^{\frac{1}{2}}=0.1$ (top) and 0.3 (bottom).

where ϵ_Ψ is given by (36). For case c,

$$E^{(\infty)}=\left[\frac{2(1-\cos\theta)}{1-2a\cos\theta+a^2}+\frac{1-a}{1+a}\langle|\epsilon_\psi^o|^2\rangle\right]^{\frac{1}{2}}, \quad (42)$$

where now $a=[1+(\kappa\lambda_\epsilon)^2]^{-1}$. The first term is associated with phase errors alone [Blumen, 1975a, Eq. (52)]; the second arises from random observational errors [Blumen, 1975b, Eq. (10)].

The asymptotic rms forecast errors for cases a and b are determined in an analogous manner using the appropriate estimates (7) and (8) at each updating period. These errors are determined from

$$\begin{aligned}\lim_{N\to\infty}(\langle|\epsilon_\Psi^{(N)}|^2\rangle)^{\frac{1}{2}}&=E^{(\infty)}\\ =\lim_{N\to\infty}\{&1-2a_{N-1}a_{N-2}\cdots a_0\cos N\theta\\ &+[a_{N-1}a_{N-2}\cdots a_0]^2(1+\langle|\epsilon_{\psi(0)}^p|^2\rangle)\\ &-2[1-a_{N-1}a_{N-2}\cdots a_0\cos N\theta][(1-a_{N-1})\cos\theta\\ &+a_{N-1}(1-a_{N-2})\cos2\theta+\cdots+(a_{N-1}\cdots a_1)\\ &\times(1-a_0)\cos N\theta]+2(a_{N-1}a_{N-2}\cdots a_0\sin N\theta)\\ &\times[(1-a_{N-1})\sin\theta+a_{N-1}(1-a_{N-1})\sin2\theta+\cdots\\ &+(a_{N-1}\cdots a_1)(1-a_0)\sin N\theta]+[(1-a_{N-1})\cos\theta\\ &+a_{N-1}(1-a_{N-2})\cos2\theta+\cdots+(a_{N-1}\cdots a_1)(1-a_0)\\ &\times\cos N\theta]^2+[(1-a_{N-1})\sin\theta+a_{N-1}(1-a_{N-2})\\ &\times\sin2\theta+\cdots+(a_{N-1}\cdots a_1)(1-a_0)\sin N\theta]^2\\ &+\langle|\epsilon_{N-1}|^2\rangle+a_{N-1}^2\langle|\epsilon_{N-2}|^2\rangle\\ &+\cdots+(a_{N-1}\cdots a_1)^2\langle|\epsilon_0|^2\rangle\}^{\frac{1}{2}}, \quad (43)\end{aligned}$$

where $(\langle|\epsilon_\psi^p(0)|^2\rangle)^{\frac{1}{2}}$ is the initial ($\tau=0$) prediction error,

$$a_n\equiv1-(1-a)\mu_{\psi(n)}-a\mu_{\pi(n)}, \quad (44)$$

$$\epsilon_n\equiv(1-a)\mu_{\psi(n)}\epsilon_\psi^o+a\mu_{\pi(n)}\epsilon_\pi^o, \quad (45)$$

and $\mu_{\psi(n)}$ and $\mu_{\pi(n)}$ are the weight factors evaluated at $n\Delta\tau$. The appropriate weight factors for cases a and b appear in Section 2. When the observational errors are related through (31),

$$\epsilon_n=a[\mu_{\pi(n)}-\mu_{\psi(n)}]\epsilon_\pi^o, \quad (46)$$

for case a. As a consequence,

$$\langle|\epsilon_n|^2\rangle=a^2(\mu_{\pi(n)}-\mu_{\psi(n)})^2\langle|\epsilon_\pi^o|^2\rangle \quad (47)$$

for $0\leqslant a\leqslant0.5$. When the observational errors are statistically independent,

$$\langle|\epsilon_n|^2\rangle=(1-a)^2\mu_{\psi(n)}^2\langle|\epsilon_\psi^o|^2\rangle+a^2\mu_{\pi(n)}^2\langle|\epsilon_\pi^o|^2\rangle. \quad (48)$$

The reduction of (43) to the asymptotic value for case c, given by (42), is carried out in the Appendix. In this limit, the asymptotic forecast error is independent of the initial error $(\langle|\epsilon_\psi^p(0)|^2\rangle)^{\frac{1}{2}}$. Also, the fact that (43) does reduce to (42) provides information on the relative magnitudes of the various errors in each of the cases. As noted by Blumen [1975a, Eq. (58)], the minimum forecast error due to phase differences, $0<\theta\leqslant\pi/3$, occurs when $a=0$. When $a=0$, $a_n=1-\mu_{\psi(n)}\neq0$ for statistically independent observational errors. However, when $a=0$, Eq. (33) shows that $\mu_{\psi(n)}=1$ so that $a_n=0$ when the observational errors are related through (31). Moreover, in this latter situation, $\langle|\epsilon_n|^2\rangle=0$ as shown by (47). On the other hand, $\langle|\epsilon_n|^2\rangle\neq0$ when $a=0$ for each of the other cases.

We may summarize these results as follows: When $0<\theta\leqslant\pi/3$, which is well within the range of model related errors ($\theta\approx0.1-0.2$)

(i) Weighted assimilation using correlated observational errors (case a) will minimize the forecast error in comparison with each of the other cases examined.

(ii) There is a trade-off when cases b and c are compared. As $a\to0$ case b is associated with larger forecast errors due to phase differences but smaller forecast errors due to observational errors, since $\mu_{\psi(n)}<1$ in (48).

These statements are illustrated in Figs. 4 and 5. The trade-off between observational errors and phase differences, noted in (ii), is evident in these figures. As the observational error increases from 0.1 to 0.3 weighted assimilation (case b) is better than the updating of case c, for all values of a, because the ratio of the observational error to the error associated with phase differences has been increased. Moreover, the computations again show the value of including appropriate dynamical constraints in the initialization procedure.

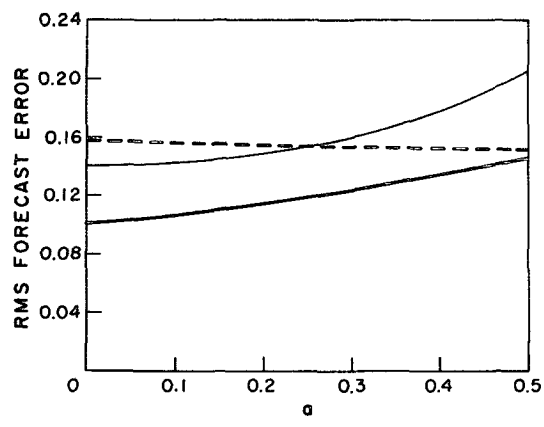

FIG. 4. Asymptotic rms forecast error, corresponding to a phase error $\theta=0.1$ and observational error $(\langle|\epsilon_\psi^o|^2\rangle)^{\frac{1}{2}}=(\langle|\epsilon_\pi^o|^2\rangle)^{\frac{1}{2}}=0.1$. The curves correspond to the three cases designated in Fig. 1 and in the text: (a) thick solid, (b) dashed and (c) thin solid.

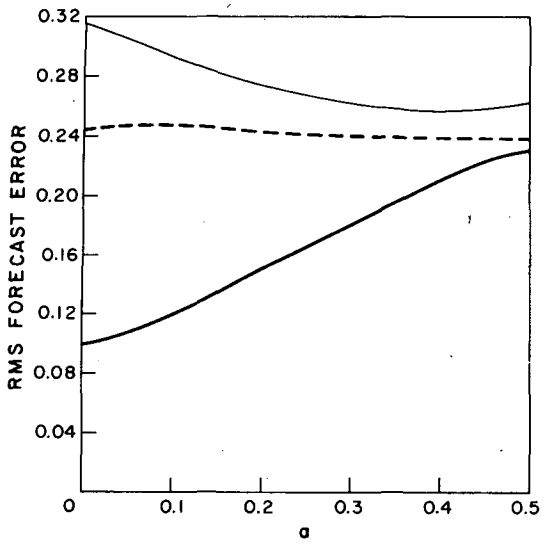

FIG. 5. As in Fig. 4 except $(\langle|\epsilon_\psi^o|^2\rangle)^{\frac{1}{2}}=(\langle|\epsilon_\pi^o|^2\rangle)^{\frac{1}{2}}=0.3$.

5. Nonlinear interactions

The present dynamical/statistical method of initialization is based on linear regression and, to some extent, linear dynamics. However, the assumption of geostrophic forecast error statistics does not, in itself, restrict the method to linear dynamical systems. The basic assumptions of potential vorticity conservation and absence of nonlinear coupling between the geostrophic and ageostrophic motions are exemplified by (2), (5) and (6). Here, the various initialization procedures that have been examined in preceding sections will be tested on a simple nonlinear triad solution that satisfies (2). It is recognized that this type of application does not violate any of the dynamical assumptions that have been built into the initialization scheme, so that an optimal performance could be anticipated. However, the effect of quadratic nonlinearities in distorting the initial error field may be brought into focus by the use of simple analytical solutions. Moreover, the role played by the initialization procedure in controlling the forecast error may also be examined in detail.

The model assumptions and method of solution are identical to those presented by Blumen (1976a). In essence, the true solution is represented by

$$\psi^t=\cos(kx+\sigma\tau+ly)+\cos(kx+\sigma\tau-ly) \quad (49)$$

and a best estimate or an observed streamfield is available for initialization. However, π^e is not given as independent information; it is calculated from the balance equation

$$\Delta\pi^e=\Delta\psi^e+2\,\mathrm{Ro}\left[\frac{\partial^2\psi^e}{\partial x^2}\frac{\partial^2\psi^e}{\partial y^2}-\left(\frac{\partial^2\psi^e}{\partial x\partial y}\right)^2\right], \quad (50)$$

where e denotes the estimate and $\mathrm{Ro}=U/f_0L\sim10^{-1}$. This method of determining initial values for the height field is not consistent with the development of the zero-order system of equations. The initial error is O(Ro). The quadratic nonlinearity in (50) give rise to an incorrect initial condition $\Psi(x,y,0)$ of the form [see Blumen (1976a, Eq. (20)]

$$\Psi(x,y,0)\approx a_1(0)\cos(kx+ly)+a_2(0)\cos(kx-ly)+a_3(0)\cos 2ly, \quad (51)$$

where a $\cos 2kx$ term has been neglected for reasons stated in the paper. The important point, for present purposes, is that condition (51) initiates a nonlinear triad solution in which two waves exchange energy over a time scale Ro τ which is the order of 10 days in dimensional units. The third wave is a stationary current, proportional to $\cos 2ly$ that acts as a catalyst enabling the propagating waves to interact. Moreover, the amplitude a_3 of the current and the frequency γ, associated with temporal changes in the wave amplitudes $a_1(\tau)$ and $a_2(\tau)$, are both proportional to the *square* of the error in the initial estimate ψ^e. This model thus provides some basic information on how nonlinearity can distort an initial error field by amplitude modulation and by introduction of a spurious wave solution, in this case a stationary current. The folowing cases will bring these remarks into clearer focus.

As noted earlier the cases treated are weighted assimilation with (a) correlated observational errors and with (b) statistically independent observational errors, and (c) use of only observations with statistically independent errors. The normalized prediction error is [Blumen, 1976a, Eq. (26)]

$$(\langle|\epsilon_\Psi|^2\rangle)^{\frac{1}{2}}=\left(\left\langle\left|\frac{\psi^t-\Psi}{\psi^t}\right|^2\right\rangle\right)^{\frac{1}{2}}=\tfrac{1}{2}\{[1-a_1(\tau)]^2+[1-a_2(\tau)]^2+a_3^2\}^{\frac{1}{2}}, \quad (52)$$

where $a_1(\tau)$, $a_2(\tau)$ and $a_3(0)$ are the wave amplitudes of the triad solution that satisfy (51) above. In cases a and b, the best estimate is provided by (7); case c corresponds to $\mu_\psi=1$ in (7). The evaluation of (52) is formally equivalent to the evaluation provided by Blumen (1976b, Section 2). In that development only observational errors were considered and the model was updated at time intervals $n\Delta\tau$; here we shall only examine the initial error growth and doubling times corresponding to initialization at one time $\tau=0(n=0)$.

The quasi-geostrophic forecast error, corresponding to each of the three cases, is

$$(\langle|\epsilon_\Psi|^2\rangle)^{\frac{1}{2}}=\{2(1-\langle\cos\gamma\tau\rangle)+\langle[(1-\mu_\psi)\epsilon_\psi^p+\mu_\psi\epsilon_\psi^o]\cos\gamma\tau\rangle+\langle[(1-\mu_\psi)\epsilon_\psi^p+\mu_\psi\epsilon_\psi^o]^2\rangle+\tfrac{1}{2}\langle[\mathrm{Ro}\,bk^2(1-(1-\mu_\psi)\epsilon_\psi^p-\mu_\psi\epsilon_\psi^o)^2]^2\rangle\}^{\frac{1}{2}}, \quad (53)$$

where (31) is used to relate the observational errors in case a and $\mu_\psi=1$ in case c. The new parameters appear-

ing in (53) are

$$\gamma = \mathrm{Ro}\,[1-(1-\mu_\psi)\epsilon_\psi^p - \mu_\psi \epsilon_\psi^o]^2 abk^3 l\lambda^2(3l^2-k^2), \quad (54)$$

$$b = (1+4l^2\lambda^2)^{-1}, \quad (55)$$

but the remaining parameters (a,λ,Ro) retain their previously established definitions. The initial growth rate is $\gamma \sim \mathrm{Ro} = 0.1$ for the characteristic values used for normalization presented in Section 3. Consequently, $\cos\gamma\tau \approx 1-(\gamma\tau)^2/2$ for the time intervals considered here. The statistical average, in (53), involves third- and fourth-order correlations. These will be neglected. The third-order correlations would vanish identically for a rectangular or normal error distribution, for example, and the fourth-order correlations, while unknown, could be expected to be relatively small.

The forecast error reduces to

$$(\langle|\epsilon_\Psi|^2\rangle)^{\frac{1}{2}} \simeq \{[\mathrm{Ro}\, abk^3 l\lambda^2(3l^2-k^2)]^2(1+6\langle\epsilon^2\rangle)\tau^2 + \langle\epsilon^2\rangle + \tfrac{1}{2}(\mathrm{Ro}\, bk^2)^2(1+6\langle\epsilon^2\rangle)\}^{\frac{1}{2}}, \quad (54)$$

where ϵ denotes the analysis error (10). Values of $\langle\epsilon^2\rangle$ for each of the cases are as follows:

CASE a

$$\langle\epsilon^2\rangle = \left(\frac{a}{1-a}\right)^2 \mu_\psi \langle|\epsilon_\pi^o|^2\rangle, \quad (55a)$$

where (32) has been introduced and μ_ψ is given by (33).

CASE b

$$\langle\epsilon^2\rangle = \mu_\psi \langle|\epsilon_\psi^o|^2\rangle, \quad (55b)$$

where μ_ψ is given by (12).

CASE c

$$\langle\epsilon^2\rangle = \langle|\epsilon_\psi^o|^2\rangle. \quad (55c)$$

The following evaluations have been made with the assumption that $\langle|\epsilon_\pi^o|^2\rangle \sim \langle|\epsilon_\psi^o|^2\rangle$, as before.

The quasi-geostrophic forecast error is composed of three terms which have simple interpretations: $\langle\epsilon^2\rangle$ is the usual analysis error as indicated above; this error is smallest for case a due to the imposed dynamical constraint; the largest value is associated with case c since $\mu_\psi < 1$ in cases a and b. The stationary term, proportional to Ro^2, is a nonlinear analysis error brought about by the presence of the spurious current in (51). Since $\langle\epsilon^2\rangle$ is a minimum for case a, the total analyses error is a minimum for case a and a maximum for case c. The nonlinear growth is represented by the first term, which is also a minimum for case a in view of the presence of $\langle\epsilon^2\rangle$ in the growth rate γ. These conclusions would carry over to periodic updating, which leads to similar forecast errors. [compare (54) with (13) in Blumen (1976b)].

A summary of results for $a=0.3$ and $a=0.5$ appears in Table 2. Values are not shown for large prediction errors when $(\langle|\epsilon_\psi^o|^2\rangle)^{\frac{1}{2}}=0.1$, since most of the weight is placed on the observations and, consequently, there is little change from the results presented for $(\langle|\epsilon_\psi^p|^2\rangle)^{\frac{1}{2}}=0.1$. Cases a and b are equivalent when $a=0.5$ but for $a<0.5$ (and $a>0.5$ by symmetry) the errors associated with case a are always smaller than the errors in either of the other cases. The time τ^* is a measure of the increase in short-range predictability due to weighted assimilation: for case c, τ^* is the doubling time of the initial analysis error due to nonlinear error growth; for cases a and b, τ^* is the time to reach the doubling error of case c; $\tau^*=1$ corresponds to one day. For example, when $(\langle|\epsilon_\pi^o|^2\rangle)^{\frac{1}{2}}=0.1$ and $a=0.3$, the initial analysis error doubles in about 12 h for case c. The same forecast error is reached about 1.5 h later for case a. As the observational error increases, predictability also increases for weighted assimilation.

TABLE 2. Root-mean-square forecast errors $(\langle|\epsilon_\Psi|^2\rangle)^{\frac{1}{2}}$ given by (54), as a function of indicated values of $a=[1+(\kappa\lambda)^2]^{-1}$ and observational and prediction errors. The column headings refer to mean square *linear* analysis error, *nonlinear* analysis error and error growth after one day; $\langle\gamma^2\rangle\tau^2=\langle\gamma^2\rangle$; and τ^* is defined in the text. Characteristic values from Section 3 have been used in the evaluation.

	$(\langle\|\epsilon_\psi^p\|^2\rangle)^{\frac{1}{2}}=0.1$, $(\langle\|\epsilon_\psi^o\|^2\rangle)^{\frac{1}{2}}=(\langle\|\epsilon_\pi^o\|^2\rangle)^{\frac{1}{2}}=0.1$				
Case	Linear	Nonlinear	$\langle\gamma^2\rangle$	$(\langle\|\epsilon_\Psi\|^2\rangle)^{\frac{1}{2}}$	τ^*
			$a=0.3$		
a	0.0016	0.0052	0.1693	0.420	0.57
b	0.0050	0.0053	0.1727	0.428	0.54
c	0.0100	0.0055	0.1778	0.440	0.51
			$a=0.5$		
a	0.0050	0.0035	0.0106	0.138	2.08
c	0.0100	0.0036	0.0109	0.156	1.93
	$(\langle\|\epsilon_\psi^p\|^2\rangle)^{\frac{1}{2}}=0.1$, $(\langle\|\epsilon_\psi^o\|^2\rangle)^{\frac{1}{2}}=(\langle\|\epsilon_\pi^o\|^2\rangle)^{\frac{1}{2}}=0.3$				
Case	Linear	Nonlinear	$\langle\gamma^2\rangle$	$(\langle\|\epsilon_\Psi\|^2\rangle)^{\frac{1}{2}}$	τ^*
			$a=0.3$		
a	0.0062	0.0053	0.1740	0.431	1.48
b	0.0090	0.0054	0.1768	0.437	1.46
c	0.0900	0.0080	0.2583	0.596	1.07
			$a=0.5$		
a	0.0090	0.0036	0.0108	0.153	5.82
c	0.0900	0.0052	0.0159	0.333	4.24
	$(\langle\|\epsilon_\psi^p\|^2\rangle)^{\frac{1}{2}}=0.3$, $(\langle\|\epsilon_\psi^o\|^2\rangle)^{\frac{1}{2}}=(\langle\|\epsilon_\pi^o\|^2\rangle)^{\frac{1}{2}}=0.3$				
Case	Linear	Nonlinear	$\langle\gamma^2\rangle$	$(\langle\|\epsilon_\Psi\|^2\rangle)^{\frac{1}{2}}$	τ^*
			$a=0.3$		
a	0.0140	0.0056	0.1817	0.449	1.43
b	0.0450	0.0066	0.2130	0.514	1.26
c	0.0900	0.0080	0.2583	0.597	1.07
			$a=0.5$		
a	0.0450	0.0043	0.0131	0.250	5.03
c	0.0900	0.0052	0.0159	0.333	4.24

In this example, weighted assimilation with correlated observational errors does not make a large impact on forecast error reduction when compared to the case with statistically independent observational errors, although some improvement is evident. In part, this result may be due to the weak nonlinear coupling assumed in this model. Consequently, the impact of dynamical/statistical initialization (case a) on the control of nonlinear error growth for short-range prediction remains an open question.

6. Remarks

The value of dynamical/statistical initialization or data assimilation has been demonstrated with a model based on conservation of potential vorticity—a principle that has been employed in the design of short-range prediction models, e.g., Bleck (1973). Of course, the acid test of any proposed initialization scheme is operational use with a primitive equation model. However, the present analysis has demonstrated that appropriate model dynamics can be incorporated into a linear regression scheme in a consistent manner. Such an inclusion "tunes" the initial analysis to the model; this desirable quality is not attained by direct use of observations nor by weighted assimilation with statistically independent observational errors.

Despite the simplicity of the present analysis, it appears safe to conclude that objective analysis schemes should be developed to produce optimal results with a particular dynamical model or should be based on physical principles that form a dynamical cornerstone of a class of models. For example, Rutherford's (1973) numerical experiments, in which statistical independence between observational errors was assumed, have led him to conclude that initialization based on the best fit to the available data does not necessarily produce the best forecast.

Although not investigated in detail here, optimal analysis and prediction can only be attained if the error statistics of various observing systems are known. However, the present results suggest that even crude estimates of these statistics are sufficient to reduce forecast error variance if the dynamics applied to the error fields is compatible with the model.

In practice, implementation of dynamical/statistical initialization in one form or another will generally add to the already complex numerics associated with the production of a forecast. For example, use of (32) requires additional computations not presently included in objective analysis schemes. Moreover, covariances between observational errors will not be confined to the diagonal of the covariance matrix, that appears in a linear regression analysis, as is the case when these errors are statistically independent. The accumulation and use of error statistics from mixed observing systems poses additional complexity, which becomes acute when measurement errors are correlated with forecast errors as, say, in the case of inversion of radiance data from satellite measurements. The present analysis has not been specifically directed to this latter problem. Nonetheless, the approach that has been taken should prove useful in the analysis of this as well as other problems relating to the dynamical control of initial error growth.

Acknowledgments. This study was initiated during the period that I was a 1975 summer visitor to the National Center for Atmospheric Research, associated with the Numerical Weather Prediction Project. I wish to thank Dr. Richard Somerville, the Project Leader, for providing the opportunity for this visit. Financial support was provided, in part, by the Atmospheric Research Section of the National Science Foundation under Grant GA-31868.

APPENDIX

Reduction of the Asymptotic Forecast Error Associated with Phase Differences

The derivation of (43) is a straightforward but long procedure and will not be displayed. As a check, (43) must reduce to (42) when $\mu_{\psi(n)}=1$ in (7) and $\mu_{\pi(n)}=0$ in (8). This corresponds to updating ψ with observed values and π with forecast values. As a consequence, a_n and ϵ_n, given by (44) and (45), reduce to

$$a_n=a, \quad \epsilon_n=(1-a)\epsilon_\psi^o. \tag{A1}$$

In the limit, $N\to\infty$, the terms a^N and a^{2N} in (43) approach zero. Consequently,

$$\begin{aligned}E^{(\infty)}=\lim_{N\to\infty}\,&[1-2(1-a)(\cos\theta+a\cos2\theta+\cdots\\&+a^{N-1}\cos N\theta)+(1-a)^2(\cos\theta+a\cos2\theta+\cdots\\&+a^{N-1}\cos N\theta)^2+(1-a)^2(\sin\theta+a\sin2\theta+\cdots\\&+a^{N-1}\sin N\theta)^2]+\lim_{N\to\infty}(1-a)^2\langle|\epsilon_\psi^o|^2\rangle\\&\times(1+a^2+a^4+\cdots).\end{aligned} \tag{A2}$$

The trigonometrical summations, in the first limit, may be found in Jolly (1961, series 499 and 500); the geometric series is given by series (4). As a result (A2) reduces to

$$\begin{aligned}E^{(\infty)}=a^{-2}&\left[1-\frac{2(1-a)(1-a\cos\theta)}{1-2a\cos\theta+a^2}+\frac{(1-a)^2}{1-2a\cos\theta+a^2}\right]\\&+\frac{(1-a)^2}{1-a^2}\langle|\epsilon_\psi^o|^2\rangle=\frac{2(1-\cos\theta)}{1-2a\cos\theta+a^2}+\frac{(1-a)}{1+a}\\&\times\langle|\epsilon_\psi^o|^2\rangle,\end{aligned} \tag{A3}$$

which is the desired expression (42).

REFERENCES

Arnold, V. I., 1965: Conditions for nonlinear stability of stationary plane curvilinear flows of an ideal fluid. *Dokl. Akad. Nauk SSSR*, **162**, 975–978. [Translation in *Sov. Math.*, **6**, 331–334.]

Bengtsson, L., 1975: 4-Dimensional assimilation of meteorological observations. GARP Publ. Ser. No. 15, WMO-ICSU Joint Organizing Committee, 76 pp. [Available from Unipub Inc., P. O. Box 433, Murray Hill Station, New York, N. Y. 10016.]

Bleck, R. 1973: Numerical forecasting experiments based on the conservation of potential vorticity on isentropic surfaces. *J. Appl. Meteor.*, **15**, 309–316.

Blumen, W., 1972: Geostrophic adjustment. *Rev. Geophys. Space Phys.*, **10**, 485–526.

——, 1975a: An analytical view of updating meteorological variables: Part I. Phase errors. *J. Atmos. Sci.*, **31**, 274–286.

——, 1975b: An analytical view of updating meteorological variables: Part II. Weighted assimilation. *J. Atmos. Sci.*, **32**, 690–697.

——, 1976a: Experiments in atmospheric predictability: Part I. Initialization. *J. Atmos. Sci.*, **33**, 161–169.

——, 1976b: Experiments in atmospheric predictability: Part II. Data Assimilation *J. Atmos. Sci.*, **33**, 170–175.

——, 1976c: A method of using multivariate statistical objective analysis to initialize a numerical prediction model. *Proc. JOC Study Group Conf. Four-Dimensional Data Assimilation*, Paris, 17–21 November 1975, 290–302. [Available from the GARP Activities Office, WMO, Geneva.]

Dikii, L. A., 1969: A variational principle in the theory of meteorological-field adaption. *Atmos. Oceanic Phys.*, **5**, 98–100.

Jolly, L. B. W., 1961: *Summation of Series*. Dover, 251 pp.

Lewis, J. M., and T. M. Grayson, 1972: The adjustment of surface wind and pressure by Sasaki's variational matching technique. *J. Appl. Meteor.*, **11**, 586–597.

Paltridge, G. W., 1975: Global dynamics and climate—a system of minimum entropy exchange. *Quart. J. Roy. Meteor. Soc.*, **101**, 475–484.

Rutherford, I. D., 1972: Data assimilation by statistical interpolation of forecast error fields. *J Atmos. Sci.*, **29**, 809–815.

——, 1973: Experiments on the updating of P. E. forecasts with real wind and geopotential data. *Preprints Third Conf. Probability and Statistics in Atmospheric Sciences*, Boulder, Amer. Meteor. Soc., 198–201.

Sasaki, Y., 1958: An objective analysis based on the variational method. *J. Meteor. Soc. Japan*, **36**, 77–88.

Schlatter, T. W., 1975: Some experiments with a multivariate statistical objective analysis scheme. *Mon. Wea. Rev.*, **103**, 246–257.

Williamson, D., and A. Kasahara, 1971: Adaptation of meteorological variables forced by updating. *J. Atmos. Sci.*, **28**, 1313–1324.